Scharf F., Mikhnevich E., Safronov A.
Chimica Techno Acta. 2017. Vol. 4, No. 2. P. 128–139.
ISSN 2409–5613

DOI: 10.15826/chimtech/2017.4.2.028

**F. Scharf[1], E. Mikhnevich[2], A. Safronov[2,3]**

*[1]TU Dresden,*
*10 Helmholtz St., Dresden, 01062, Germany*
*e-mail: scharf.franziska@gmail.com*
*[2]Ural Federal University,*
*19 Mira St., Ekaterinburg, 620002, Russia*
*E-mail: koyoto4ka@rambler.ru*
*[3]Institute of Electrophysics UB RAS,*
*106 Amundsen St., Ekaterinburg, 620016, Russia*
*E-mail: safronov@iep.uran.ru*

# Interaction of iron oxide nanoparticles synthesized by laser target evaporation with polyacrylamide in composites and ferrogels

Iron oxide magnetic nanoparticles (MNPs) with average diameter 11.7 nm synthesized by laser target evaporation were used for the synthesis of composites and ferrogels based on polyacrylamide network. The chemical composition of MNPs corresponded to maghemite. It was shown that intact MNPs strongly interacted with polyacrylamide polymeric network, while the adsorption of electrostatic stabilizer on the surface of MNPs efficiently prevents such interaction. Synthesis of ferrogels was performed by the radical polymerization of acrylamide in electrostatically stabilized suspensions of MNPs in water. It was shown that the molecular structure, water uptake, and compression modulus can be controlled by the concentration of monomer taken in the synthesis.

**Keywords:** nanoparticles; iron oxide; composites; ferrogels; polyacrylamide

Received: 05.06.2017; accepted: 20.06.2017;published: 14.07.2017.



## Introduction

Novel advanced polymeric composites with embedded magnetic particles attract special attention due to their prospective applications in biomedical applications, which include magnetic sensors, actuators, and systems for the controlled drug delivery [1–3]. Such materials are based on the matrix of a biocompatible polymer with magnetic particles, which are embedded into it. Iron oxides – magnetite and maghemite are widely used for this purpose. Considering the practical application in biomedicine and bioengineering it is important to ensure well controlled shape of iron oxide particles and a large single batch of their production. The fabrication techniques providing enhanced batch sizes [4, 5] attract special attention as the properties of MNPs can vary from batch to batch. One of the methods of MNPs synthesis providing a high production rate is the physical method of the

laser target evaporation (LTE) [6–9]: it provides 10 to 50 nm spherical MNPs at ca. 100 g per hour production rate.

A magnetic polymeric composite for biomedical application might be a two-component system, which consists of a polymeric matrix and dispersed magnetic particles, and as well might be a three-component system which contains water in its structure as well. In the latter case the composite is called ferrogel. The polymeric matrix of a ferrogel constitutes of chemically and of physically cross-linked polymeric network swollen in water. Water-based gels (hydrogels) are extensively studied as biocompatible and biomimetic materials which closely resembles not only the molecular structure of biological tissues but the response of these tissues to such stimuli as pH, temperature, salt concentration as well [10, 11]. Polyacrylamide (PAAm) is often used for the synthesis of ferrogels with iron oxide MNPs [12–14]. PAAm is a water soluble biocompatible polymer and it can form chemically cross-linked networks of homogeneous hydrogels with the network density varying in a broad range. The application of PAAm ferrogels as a potential material for biosensors had been demonstrated [15]. The conventional approach in the studies on polyacrylamide ferrogels is focused on their magnetic properties and their response to the applied magnetic field. It is obvious that the response of a polymeric composite material like ferrogel depends not only on the magnetic properties of the dispersed MNPs but also on their interaction with polymeric matrix. Meanwhile, the studies on the interactions at the interface between polymer and embedded solid particle in composites and ferrogels are lacking.

The main objective of this paper was to analyze interaction of polyacrylamide with embedded iron oxide nanoparticles in a binary composite and in ternary systems including ferrogels. The adsorption of polyacrylamide polymeric chains from water solutions on the surface of iron oxide MNPs as well as the enthalpy of interaction at the interface was studied. It gave the basis for the analysis of the molecular structure of polyacrylamide ferrogel and its basic properties: uptake of water (the swelling degree) and the compression modulus, which to a large extent govern its biomedical applicability.

## Experimental: Materials

*Iron oxide MNPs*

Iron oxide (FeOx) magnetic nanoparticles (MNP) were synthesized by laser target evaporation (LTE) – the method of high temperature physical dispersion based on the evaporation of a solid pellet by the laser beam with consequent condensation of vapors in the gas phase. LTE was performed using laboratory installation with Ytterbium (Yb) fiber laser with 1.07 μm wavelength operated in a pulsed regime with pulse frequency 4.85 kHz and pulse duration 60 μs. Average output power of irradiation was about 212 W. The target pellet 65 mm in diameter, 20 mm in height was made of the commercial magnetite ($Fe_3O_4$) (Alfa Aesar, Ward Hill, MA, USA) powder (specific surface area 6.9 $m^2/g$). The laser beam was focused onto the target pellet surface by optical system Optoscand d25 f60/200 with 200 mm focal length. The driving mechanism provided 20 cm/s beam scan rate on the target surface, which ensured uniform wear-out of the target surface. The working gas (a mixture of $N_2$ and $O_2$

in the volume ratio 0.79:0.21) was blown into the evaporation chamber by the fan. The oxide vapors were driven away from the focal spot and condensed in spherical nanoparticles.

*Polyacrylamide/FeOx magnetic composites*

Linear polyacrylamide (LPAAm) which served as a polymeric matrix for the magnetic composites was synthesized by the radical polymerization reaction of acrylamide (AAm) (AppliChem, Darmstadt) in 1.6 M water solution at 80 °C. Ammonium persulfate (PSA) in 5 mM concentration was used as an initiator. The reaction mixture was kept at 80 °C for 1h. The obtained LPAAm solution was then diluted with distilled water down to 5 % concentration by weight. The resulted solution was then used as a stock for the preparation of magnetic composites. The molar weight of LPAAm determined by viscometry was $M = 1.0 \cdot 10^6$ g/mol.

The stock solution of LPAAm was used for the preparation of LPAAm/FeOx magnetic composites. Therefore MNPs were mixed with the stock solution in the pre-calculated proportions to obtain composites with different LPAAm/FeOx ratios, which cover the entire composition range 0–100 % of FeOx at 10 % steps. Weighted sample of dry powder was wetted by a few drops of water and vigorously stirred in a mortar. Then the weighted amount of 5 % LPAAm stock solution was added. The mixed suspension was stirred in a mortar to homogeneity and then cast onto PTFE plate. The cast mixture was then dried in an oven at 85 °C down to the constant weight, and the composite films of different LPAAm/FeOx ratio were obtained.

*Ferrogels*

Prior to the synthesis of ferrogels a stable ferrofluid of MNPs in water was obtained. Therefore FeOx was suspended into 5 mM sodium citrate solution. The suspension was subjected to an ultra-sonic treatment for dispersion. The process of MNPs de-aggregation every 15 minutes was monitored by the dynamic light scattering (DLS). As soon as hydrodynamic diameter did not change any more significantly, the suspension was placed in a centrifuge at 9000 rpm for 5 minutes to remove remaining aggregates. The final suspension had an effective hydrodynamic diameter 65.7 nm (intensity average). The weight concentration of the MNPs in suspension was estimated to 8.66 % by drying a sample of the ferrofluid.

Ferrogels were synthesized by the radical polymerization of AAm in the obtained ferrofluid. The total concentration of AAm in the reaction mixture was kept at two levels: 0.8 M and 1.6 M, which formed two series of ferrogels with increasing content of FeOx MNPs up to 4 % (wt). Methylene diacrylamide (Merck, Schuchardt) was used as a cross-linker in a molar ratio 1:100 to AAm. Ammonium persulfate was used as an initiator in 5 mM concentration. To start and to accelerate the polymerization, few droplets of the catalyst TEMED (Sigma-Aldrich) were added to the reaction mixture. Then it was filled into plastic molds closed with Parafilm. The synthesis lasted 1h at 25 °C. After that the ferrogels were taken out from the molds and placed in glass containers filled with distilled water and they were kept in it for two weeks period with daily water renewal. During this period the gels were swollen to the equilibrium.

## Experimental: Methods

The powder X-ray diffraction (XRD) patterns were recorded on Bruker D8 Discover with Cu $K_{\alpha 1.2}$ radiation ($\lambda$ = 1.542 Å) with graphite monochromator. The Rietveld refinement of XRD patterns were performed using Topas-3 software. The morphology of MNPs was examined using JEOL JEM2100 transmission electron microscope (TEM) operating at 200 kV. The specific surface area of MNPs was measured by the low-temperature adsorption of nitrogen (Brunauer-Emett-Teller (BET) approach) using Micromeritics TriStar3000 analyzer. Dynamic light scattering (DLS) and electrophoretic light scattering (ELS) measurements were performed using Brookhaven ZetaPlus particle size analyzer: 5 and 3 runs were recorded for hydrodynamic size and zeta-potential measurements, respectively. The adsorption of LPAAm on the surface of FeOx from water solutions was estimated from the difference of LPAAm concentration before and after the adsorption measured with the use of the refractometer Atago DR-1A. Calibration was done using LPAAm solutions with increasing concentration. Microcalorimetry measurements of the enthalpy of dissolution of LPAAm/FeOx composites in distilled water were performed at 25 °C using SETARAM C80 microcalorimeter. The glass ampoule technique was elaborated. The weighted sample of composite film (20–40 mg) in a thin glass ampoule was placed in a stainless steel cell filled with 10 mL of distilled water. After thermal equilibration the ampoule was broken by a special rod and the enthalpy of dissolution was measured with 2 % accuracy. The equilibrium swelling degree of ferrogels was determined as a ratio of the content of water in the gel to the weight of the dry residue which was measured gravimetrically. The swelling degree was corrected by the weight percentage of MNPs in the ferrogel. The compression modulus was measured using a laboratory setup providing compressive loading of gel samples and their simultaneous optical registration during deformation.

## Results and their discussion

Fig. 1 presents TEM image of FeOx MNPs synthesized by laser target evaporation. They are spherical in shape and non-aglomerated. The particle size distribution (PSD) fits well the following log-normal equation:

$$PSD(d) = \frac{2.46}{d} e^{-\frac{(\ln d - \ln(11.7))^2}{2 \cdot 0.423^2}} \qquad (1)$$

The specific surface area of MNPs ($S_{sp}$) measured by the low-temperature adsorption of nitrogen was 78 $m^2/g$. The surface average diameter of MNPs, calculated from this value using the equation $d_s = 6/(\rho S_{sp})$ ($\rho$ = 4.6 $g/cm^3$ being iron oxide density) was 16.7 nm. It was in a good agreement with the value $d_s$ = 15.9 nm, obtained using equation (1).

Fig. 2 presents XRD plot for FeOx MNPs. The crystalline structure of MNPs corresponded to the inverse spinel lattice with a space group Fd3m. The lattice period was found $a$ = 0.8358 nm, which was larger than that for maghemite ($\gamma$-$Fe_2O_3$, $a$ = 0.8346 nm) but lower than that for magnetite ($Fe_3O_4$, $a$ = 0.8396) [16] Based on the dependence between the lattice period of the spinel cell and the effective state of oxidation of Fe the composition of MNPs contained 76 % of $\gamma$-$Fe_2O_3$, and

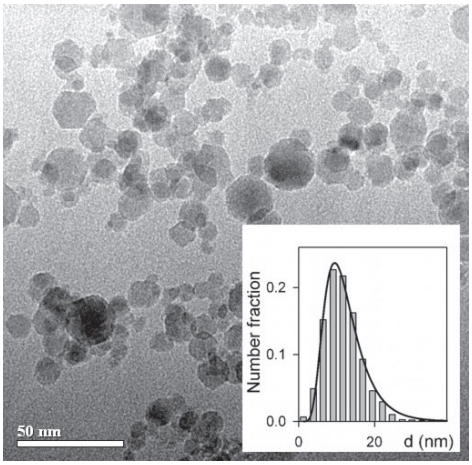


Fig. 1. TEM image of FeOx magnetic nanoparticles synthesized by laser target evaporation. Inset: histogram – calculation of particle number fraction from the image analysis, line – fitting of PSD by equation (1)

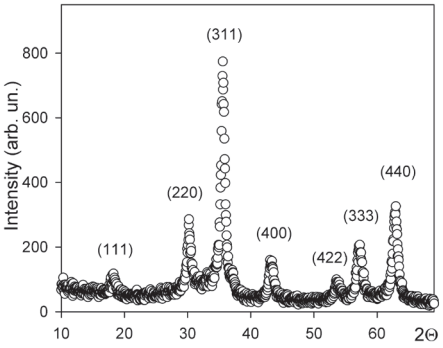


Fig. 2. XRD diffractogram of FeOx MNPs synthesized by laser target evaporation

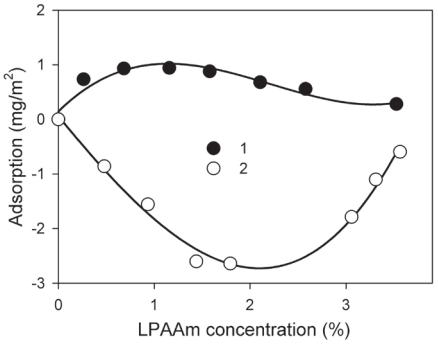


Fig. 3. Adsorption of LPAAm on FeOx MNPs from water solution at 25 °C. 1 – intact FeOx surface; 2 – Citrate covered FeOx surface

24 % of $Fe_3O_4$. The coherence length of monocrystalline domains estimated using the Scherrer approach was 11 nm. This value correlates well with the median value of PSD (11.7 nm) obtained by TEM.

The isotherms of the adsorption of LPAAm on the surface of FeOx from water solutions at 25 °C are depicted in Fig. 3.

Curve 1 in Fig. 3 corresponds to the case if the adsorption occurs on the surface of non-stabilized FeOx MNPs which is presumably formed by iron oxide crystalline lattice. Curve 2 corresponds to a quite common case if electrostatic stabilizer NaCit was used to provide the stability of MNPs in suspension. In the latter case the surface of MNPs is covered by adsorbed citrate anions. These two cases were found to be significantly different considering the adsorption of LPAAm.

Let us first discuss the adsorption on the intact oxide surface (Fig. 3, Curve 1). It is recognizable that the adsorption depends on the concentration of PAAm. In the range of PAAm concentration from 0 % to ca. 1.5 % the measured adsorption increases. At concentrations higher than ca. 1.5 % it is declining. The course of the curve is characteristic for moderate concentrated solutions of linear flexible macromolecules. In solution such chains have a conformation of a coil, which is an equilibrium one for a flexible polymer. At low concentration these coils do not overlap with each other and can adsorb on the particle surface separately. The typical threshold of coil overlapping is around 1–2 %. At concentration above the threshold LPAAm coils are overlapping and their adsorption decreases due to the steric limitations.

The results of the adsorption measurement with the surface of FeOx covered with citrate as a stabilisator are very dif-

ferent (Fig. 3, Curve 2). In contrary to the case of the intact FeOx surface, all the values of the measured adsorption are negative. The lowest value is reached at ca 2 % concentration of LPAAm. It is worth to note that the values of adsorption correspond to the excess of the concentration of the adsorbing molecules over the average concentration in the system. Thus the negative values of the adsorption simply mean that the content of LPAAm in the layer attached to the surface of MNPs in lower than that in the bulk solution. In other words it means that the PAAm molecules are repelled by the surface of the iron oxide particles. The concentration of PAAm in access of MNPs is lower than at places where no MNPs are. NaCit is subjected to be decisive for the repulsion of PAAm. By the use of NaCit the suspension was stabilized and particles were covered with a double electrical layer. It might be assumed that the electrical layer causes the repulsion of PAAm.

To clarify the influence of surface nature on the interaction between LPAAm and FeOx MNPs, calorimetric study on the enthalpy of interaction between LPAAm and MNPs was performed. By these measurements the enthalpy of mixing $\Delta H_m$ was calculated for model composites LPAAm/FeOx. The model composites were made once in the presence of NaCit and once in the absence.

The enthalpy ($\Delta H_m$) of mixing for the polyacrylamide composite filled with iron oxide MNPs has to be calculated, because it is not measurable directly. For the calculation the thermochemical cycle is used [17]. It includes the following steps:

1) LPAAm + $H_2O$ (excess) = LPAAm dilute solution + $\Delta H_1$

2) FeOx + $H_2O$ (excess) = FeOx ferrofluid + $\Delta H_2$

3) LPAAm/FeOx + $H_2O$ (excess) = = LPAAm solution in ferrofluid + $\Delta H_3$

4) LPAAm solution + ferrofluid = = LPAAm solution in ferrofluid + $\Delta H_4$

Combination of these steps gives the following equation for the formation of the composite from the components:

$$\text{LPAAm + FeOx = } \\ = \text{LPAAm/FeOx composite} + \Delta H_m \quad (2)$$

According to Hess law the enthalpy of mixing is the following combination of enthalpies of the steps:

$$\Delta H_m = \omega_1 \Delta H_1 + \omega_2 \Delta H_2 + \\ + \Delta H_3 - \Delta H_4, \quad (3)$$

here $\omega_1$, $\omega_2$ – are the weight fractions of LPAAm and FeOx in composite.

The calculated values of $\Delta H_m$ correspond to the temperature at which calorimetry measurements were performed (25 °C).

Fig. 4 presents the dependence of $\Delta H_3$ values, which were measured directly in calorimeter, on the weight fraction of FeOx MNPs in composite.

The values of the enthalpy of dissolution ($\Delta H_3$) are negative in all cases. The value at zero weight concentration of MNPs corresponds to the enthalpy of dissolution of pure LPAAm ($\Delta H_1$). It is

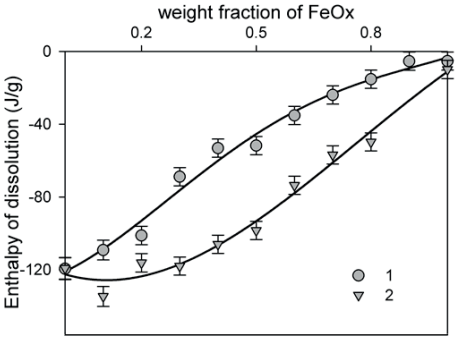


Fig. 4. Enthalpy of dissolution of LPAAm/FeOx composite in water at 25 °C.
1 – FeOx MNPs with intact surface; 2 – FeOx MNPs treated with sodium citrate. Lines are for eye-guide only

strongly exothermic – 120 J/g. The enthalpy of wetting of FeOx MNPs ($\Delta H_2$) is low, –5.5 J/g. With increasing of weight fraction ($\omega_2$) of MNPs the enthalpy of dissolution declines. At $\omega_2 = 1$ it is equal to $\Delta H_3$. It is noticeable that the dependences of the enthalpy of dissolution for the composites with intact FeOx and citrate-covered FeOx are different. The values of $\Delta H_3$ in the latter case are more negative.

The results of the calculation $\Delta H_m$ using equation (3) are presented in Fig. 5. It is apparent that the enthalpy of mixing strongly depends on the surface of FeOx MNPs which are interacting with LPAAm chains. In case of FeOx MNPs with intact surface the values of $\Delta H_m$ are negative in the broad composition range (weight fraction 0.2–1.0), whereas they are positive over the entire composition range if the surface of FeOx MNPs is covered with citrate. This result is consistent with the adsorption measurements presented above. Based on thermochemical data we may conclude that negative adsorption of LPAAm at the surface of FeOx MNPs covered with citrate is the result of positive enthalpy of interaction at the surface.

Experimental data in Fig. 5 were fitted by the thermodynamic model developed for the polymeric composites filled with solid particles [18]

$$\Delta H_{\mathrm{m}} = \Delta H_{ads}^{\infty} \frac{K(1-\omega_2)\omega_2 S_{sp}}{K(1-\omega_2)+S_{sp}\omega_2} - \\ -\varepsilon_{coh}\varphi_{pol}\gamma \exp\left(-\frac{1-\omega_2}{S_{sp}\omega_2\rho_{pol}L}\right) \quad . \quad (4)$$

Here $\Delta H_{ads}^{\infty}$ is the characteristic enthalpy of polymer adsorption at the solid surface per 1 m$^2$, $K$ is the apparent constant of adsorption, $\varepsilon_{coh}$ is the cohesion enthalpy of polymer matrix per 1 g of polymer, $\varphi_{pol}$ is the volume fraction of polymer in composite, $\rho_{pol}$ is the density of polymer, $L$ is the characteristic thickness of the adsorption layer, $\gamma$ is the excess fraction of metastable voids in the glassy structure of polymer at the surface.

Solid lines in Fig. 5 are the results of fitting of experimental data by equation (3). Concerning the objective of the present study the fitting parameter $\Delta H_{ads}^{\infty}$ is of major importance as it stands for the interaction at the surface. The fitting procedure gave the values –10.5 and +14.7 J/m$^2$ for the adsorption of LPAAm at the intact FeOx surface and at the surface covered with citrate respectively. These values might be taken as quantitative evaluation for the difference between enthalpy of interaction of LPAAm with these two types of surfaces.

Based on the presented results on the interaction between FeOx MNPs and polyacrylamide let us consider the properties of ferrogels, which constitute the network of PAAm chains with embedded FeOx MNPs. The question, which immediately arises while considering ferrogels is whether MNPs can or can not change their location inside the network. In prin-

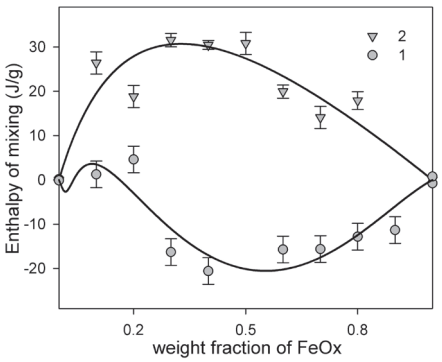


Fig. 5. Enthalpy of mixing of LPAAm/FeOx composites at 25 °C: 1 – FeOx MNPs with intact surface; 2 – FeOx MNPs treated with sodium citrate. Lines correspond to fitting of experimental data by equation (3)

ciple, there are two factors that influence the mobility of MNPs: the mesh size of the network and the adhesion of MNPs to the subchains of the network. As for the latter, it was clearly shown above that interaction of PAAm chains to the surface of FeOx MNPs strongly depended on the nature of the surface. If MNPs with intact surface would be used in ferrogels one might assume strong adhesion of subchains to the surface. In case of citrate-coated MNPs, on the contrary, one would expect no adhesion of subchains to the surface of MNPs.

In fact, electrostatic stabilization by sodium citrate is the most common way to prevent aggregation of ferrofluid in preparation of ferrogels. We have used the same procedure in the synthesis of ferrogels in the present study (see Materials section). Thus, in the ferrogels we have synthesized FeOx MNPs were not interacting with PAAm subchains.

As for the mesh size of the network, it can be estimated based on the equilibrium swelling degree of a gel, which is the uptake of water by the dry polymeric network. The degree of swelling related solely to the polyacrylamide network in ferrogels was 30.0 if the concentration of AAm in synthesis was 0.8 M and it was 13.2 if such concentration was 1.6 M. Based on the equilibrium degree of swelling of polymeric network ($\alpha$) the average number of monomer units in linear sub-chains between cross-links ($N_C$) was evaluated using Flory-Rehner equation [19]:

$$N_C = \frac{V_1(0.5\alpha^{-1} - \alpha^{-1/3})}{V_2(\ln(1-\alpha^{-1}) + \alpha^{-1} + \chi\alpha^{-2})}, \quad (5)$$

where $V_1$, $V_2$ – are molar volumes of solvent and of polymer respectively, $\chi$ – is Flory-Huggins parameter for a polymer – solvent mixture. We used $V_1$=18 cm$^3$/mol (water), $V_2$ = 56.2 cm$^3$/mol (polyacrylamide) and $\chi$ = 0.12. The last two values were obtained by means of quantum mechanics molecular modeling software package CAChe7.5. Equation (5) gave the number of monomer units in linear subchains $N_C$ = 225 if AAm concentration was 0.8 M and $N_C$ = 53 if AAm concentration was 1.6 M.

The equilibrium conformation of electrically neutral polyacrylamide subchain in water is a random Gaussian coil with hindered rotation. Its mean square end-to-end distance $\langle R^2 \rangle$, which corresponds to the distance between adjacent cross-links can be calculated according to the equation [20]:

$$\left\langle R^2 \right\rangle = Na^2 \frac{1-\cos\vartheta}{1+\cos\vartheta}, \quad (6)$$

where $N$ is the number of bonds in the polymeric chain, $a$ is the bond length, $\theta$ is the bond angle. We took $a$ = 0.154 nm for the ordinary C–C bond, $\theta$ =109.5° for the bond angle, and $N = 2N_C$ for the number of bonds (it is two fold larger than $N_C$ as it includes the bonds in monomer units and bonds between them). The distance between the cross-links, calculated using equation (6) is 10.6 nm for the network synthesized in 0.8 M AAm and it is 1.6 nm for the network synthesized in 1.6 M solution of AAm. The former value is close to the average diameter of MNPs (11.7 nm), the latter value is substantially smaller. It means that the molecular structure of two series of ferrogels is different. The essential structural features of studied polyacrylamide/FeOx ferrogels may be illustrated by Fig. 6. Further on these two types of ferrogels will be denoted as 0.8 M series and 1.6 M series.

Fig. 7 presents the swelling degree of PAAm ferrogels in the dependence on the content of FeOx MNPs. It is noticeable that the swelling degree of ferrogels

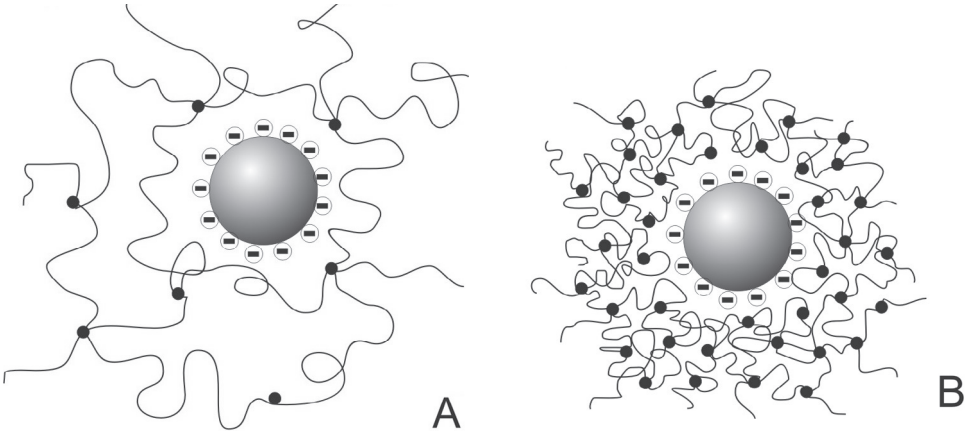


Fig. 6. Schematic presentation of molecular structure of polyacrylamide ferrogels with citrate-coated FeOx MNPs: A – 0.8 M series; B – 1.6 M series. Lines schematically show polyacrylamide subchains in the network, black dots indicate the crosslinks

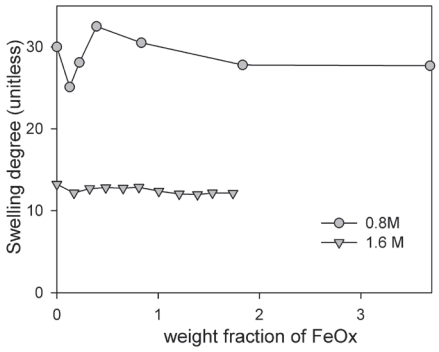


Fig. 7. Swelling degree of PAAm ferrogels with citrate-covered FeOx MNPs. Circles –0.8 M series, triangles –1.6 M series

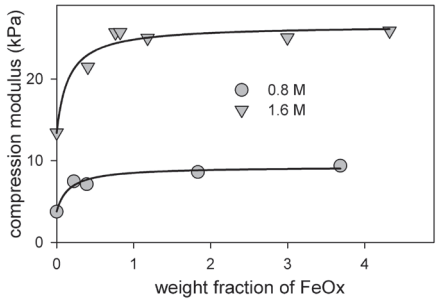


Fig. 8. Compression modulus of PAAm ferrogels with citrate-covered FeOx MNPs. Circles –0.8 M series, triangles 1.6 M series

of 0.8 M series is higher than in the case of 1.6 series. It is due to the larger mesh size of the network in the former case as it was shown above. It is worth to mention that the swelling degree corresponds exclusively to PAAm network among MNPs. Although the subchains do not adsorb on the surface of MNPs, their presence influences the swelling. It gives a certain dependence of the swelling degree on the weight fraction of FeOx MNPs. This dependence is more evident in 0.8 M series of ferrogels. The first portion of MNPs diminishes the swelling degree. Then it increases, goes through the maximum and gradually decreases. The same dependence can be noticed in case of 1.6 M series but the variation is close to the experimental error.

Fig. 8 presents the compression modulus of the ferrogels of both series. There is the same trend for the dependence on weight fraction of MNPs: the modulus strongly increases at the first portions of MNPs embedded in the gel network and then comes to saturation. The initial raise up of modulus is quite substantial: the

embedding of 0.5 % of FeOx MNPs, which correspond to ca. 0.1 % volume fraction, resulted in two-fold elevation of modulus above the value for the PAAm hydrogel without MNPs. Such a trend certainly contradicts with the conventional consideration of the modulus of continuous medium (E) with dispersed solid spheres based on the Einstein equation:

$$E = E_0\left(1+\frac{5}{2}\varphi\right), \quad \varphi << 1 \qquad (7)$$

The reasons for this effect are not clear so far. Meanwhile, it is noticeable that the initial raise up of the modulus correlates with the decrease of the swelling degree of ferrogel, so one may assume the connection between them.

The influence of the network density on the modulus is quite reasonable: the dense network of ferrogels of 1.6 M series (see Fig. 6) provide much higher values of modulus as compared to the loose network of ferrogels of 0.8 M series.

## Conclusions

Iron oxide magnetic nanoparticles (FeOx MNPs) synthesized by laser target evaporation can be succefully embedded in composites and ferrogels based on polyacrylamide (PAAm). The enthalpy of interaction between the surface of MNPs and PAAm depends strongly on the pretreatment of MNPs. In the case of the intact FeOx particles taken *per se* the interaction is strong and the adsorption of PAAm chain onto the surface takes place. Meanwhile, if the surface of MNPs is coated with citrate anions, which act as a common electrostatic stabilizer for FeOx suspensions, interaction of PAAm with the surface vanishes: the enthalpy of interaction becomes positive and PAAm chains are repelled from the surface. However, the use of citrate might be necessary to provide the synthesis of PAAM ferrogels in the stable ferrofluids of FeOx MNPs. The network density of such ferrogels, their water uptake, and the compression modulus can be efficiently controlled by the concentration of AAm monomer in the reaction mixture. The increase in AAm concentration from 0.8 M up to 1.6 M results in ten-fold decrease in mesh-size of the network, in 2.5-fold decrease in the swelling degree and in 2.5-fold elevation of the compression modulus.

## References


1. Llandro J, Palfreyman JJ, Ionescu A, Barnes CHW. Magnetic biosensor technologies for medical applications: A review. *Med Biol Eng Comput.* 2010;48(10):977–8. DOI:10.1007/s11517–010–0649–3.
2. Hamidi M, Azadi A, Rafiei P. Hydrogel nanoparticles in drug delivery (Review). *Adv Drug Delivery Rev.* 2008;60(15):1638–49. DOI:10.1016/j.addr.2008.08.002.
3. Li Y, Huang G, Zhang X, Li B, Chen Y, Lu T, Lu TJ, Xu F. Magnetic Hydrogels and Their Potential Biomedical Applications. *Adv Func Mater.* 2013;23(6):660–72. DOI:10.1002/adfm.201201708.
4. Grossman JH, McNeil SE. Nanotechnology in cancer medicine. *Phys Today*. 2012;65(8):38–42. DOI:10.1063/PT.3.1678.

5. Malumbres A, Martínez G, Mallada R, Hueso JL, Bomatí-Miguel O, Santamaría J. Continuous production of iron-based nanocrystals by laser pyrolysis. Effect of operating variables on size, composition and magnetic response. *Nanotechnology*. 2013;24(32):325603. DOI:10.1088/0957–4484/24/32/325603.
6. Muller E, Oestreich Ch, Popp U, Michel G, Staupendahl G, Henneberg KH. Characterization of Nanocrystalline Oxide Powders Prepared by $CO_2$ Laser Evaporation. *KONA Powder Part J.* 1995;13:79–90. DOI:10.14356/kona.1995012.
7. Kurland HD, Grabow J, Staupendahl G, Andra W, Dutz S, Bellemann ME. Magnetic iron oxide nanopowders produced by $CO_2$ laser evaporation. *J Magn Magn Mater*. 2007;311(1):73–7. DOI:10.1016/j.jmmm.2006.10.1166.
8. Osipov VV, Platonov VV, Uimin MA, Podkin AV. Laser synthesis of magnetic iron oxide nanopowders. *Tech Phys.* 2012;57(4):543–9. DOI:10.1134/S1063784212040214.
9. Safronov AP, Beketov IV, Komogortsev SV, Kurlyandskaya GV, Medvedev AI, Leiman DV, Larranaga A, Bhagat SM. Spherical magnetic nanoparticles fabricated by laser target evaporation. *AIP Advances*. 2013;3(5):052135. DOI:10.1063/1.4808368.
10. Ling GN. Revolution in the Physiology of the Living Cell. Malabar (FL): Krieger Publishing; 1992. 378 p.
11. Pollack GH. Cells, Gels and the Engines of Life. Seattle: Ebner&Sons; 2001. 305 p.
12. Galicia JA, Sandre O, Cousin F. Designing magnetic composite materials using aqueous magnetic fluids. *J Phys: Condens Matter*. 2003;15(15):1379–402. DOI:10.1088/0953–8984/15/15/306.
13. Galicia JA, Cousin F, Dubois E, Sandre O, Cabuil V, Perzynski R. Static and dynamic structural probing of swollen polyacrylamide ferrogels. *Soft Matter*. 2009;5(13):2614–24. DOI:10.1039/b819189a.
14. Galicia JA, Cousin F, Dubois E, Sandre O, Cabuil V, Perzynski R. Local structure of polymeric ferrogels. *J Magn Magn Mater.* 2011;323(10):1211–5. DOI:10.1016/j.jmmm.2010.11.008.
15. Kurlyandskaya GV, Fernandez E, Safronov AP, Svalov AV, Beketov I, Burgoa Beitia A, Garcıa-Arribas A, Blyakhman FA. Giant magnetoimpedance biosensor for ferrogel detection: Model system to evaluate properties of natural tissue. *Appl Phys Lett*. 2015;106(19):193702. DOI:10.1063/1.4921224.
16. Pearson WB. Handbook of lattice spacing structures of metals and alloys. London: Pergamon Press; 1958. 1044 p.
17. Shankar A, Safronov AP, Mikhnevich EA, Beketov IV, Kurlyandskaya GV. Ferrogels based on entrapped metallic iron nanoparticles in a polyacrylamide network: extended Derjaguin–Landau–Verwey–Overbeek consideration, interfacial interactions and magnetodeformation. *Soft Matter*. 2017;13:3359–72. DOI:10.1039/C7SM00534B.
18. Safronov AP, Istomina AS, Terziyan TV, Polyakova YI, Beketov IV. Influence of Interfacial Adhesion and the Nonequilibrium Glassy Structure of a Polymer on the Enthalpy of Mixing of Polystyrene-Based Filled Composites. *Polym Sci, Ser A*. 2012;54(3):214–23. DOI:10.1134/S0965545X12030108.

19. Quesada-Perez M, Maroto-Centeno JA, Forcada J, Hidalgo-Alvarez R. Gel swelling theories: The classical formalism and recent approaches. *Soft Matter*. 2011;7(22):10536–47. DOI:10.1039/c1sm06031g.
20. Rubinstein M, Colby RH. Polymer physics. New York: Oxford University Press; 2003. 442 p.

**Cite this article as (как цитировать эту статью)**
Scharf F, Mikhnevich E, Safronov A. Interaction of iron oxide nanoparticles synthesized by laser target evaporation with polyacrylamide in composites and ferrogels. *Chimica Techno Acta*. 2017;4(2):128–139. DOI: 10.15826/chimtech.2017.4.2.028.